Atmos. Chem. Phys. Discuss., 13, 5123–5163, 2013
www.atmos-chem-phys-discuss.net/13/5123/2013/
doi:10.5194/acpd-13-5123-2013

Atmospheric Chemistry and Physics Discussions

Evaluation of spatio-temporal variability of Hamburg Aerosol Climatology against aerosol datasets from MODIS and CALIOP

V. Pappas[1], N. Hatzianastassiou[1], C. Papadimas[1], C. Matsoukas[2], S. Kinne[3], and I. Vardavas[4]

[1]Laboratory of Meteorology, Department of Physics, University of Ioannina, 45110 Ioannina, Greece
[2]Department of Environment, University of the Aegean, 81100 Mytilene, Greece
[3]Max-Planck Institute for Meteorology, 20146 Hamburg, Germany
[4]Department of Physics, University of Crete, 71110 Heraklion, Crete, Greece

Received: 24 November 2012 – Accepted: 21 January 2013 – Published: 22 February 2013

Correspondence to: N. Hatzianastassiou (nhatzian@cc.uoi.gr)

Published by Copernicus Publications on behalf of the European Geosciences Union.

Abstract

The new global aerosol climatology named HAC (Hamburg Aerosol Climatology) is compared against MODIS (MODerate resolution Imaging Spectroradiometer, Collection 5, 2000–2007) and CALIOP (Cloud-Aerosol Lidar with Orthogonal Polarization, Level 2-Version 3, 2006–2011) retrievals. The HAC aerosol optical depth (AOD) values are larger than MODIS in heavy aerosol load conditions (over land) and lower over oceans. Agreement between HAC and MODIS is better over land and for low AOD. Hemispherically, HAC has 16–17 % smaller AOD values than MODIS. The discrepancy is slightly larger for the Southern Hemisphere (SH) than for the Northern Hemisphere (NH). Seasonally, the largest absolute differences are from March to August for NH and from September to February for SH. The spectral variability of HAC AOD is also evaluated against AERONET (1998–2007) data for sites representative of main aerosol types (pollutants, sea-salt, biomass and dust). The HAC has a stronger spectral dependence of AOD in the UV wavelengths, compared to AERONET and MODIS. For visible and near-infrared wavelengths, the spectral dependence is similar to AERONET. For specific sites, HAC AOD vertical distribution is compared to CALIOP data by looking at the fraction of columnar AOD at each altitude. The comparison suggests that HAC exhibits a smaller fraction of columnar AOD in the lowest 2–3 km than CALIOP, especially for sites with biomass burning smoke, desert dust and sea salt spray. For the region of the greater Mediterranean basin, the mean profile of HAC AOD is in very good agreement with CALIOP. The HAC AOD is very useful for distinguishing between natural and anthropogenic aerosols and provides high spectral resolution and vertically resolved information.

1 Introduction

During the last decades, the scientific community has been trying to estimate the sign and magnitude of the well-established factors contributing to the net climate change

ACPD
13, 5123–5163, 2013

since pre-industrial times. One of the greatest uncertainties in the overall present picture lies in the interaction between clouds, aerosols and radiation (IPCC, 2007) especially, the effects of the highly variable aerosol optical properties. Aerosols scatter and absorb solar radiation, reducing the amount reaching the surface and warming the atmosphere. This can have impacts on evaporation from the surface, and also in cloud formation and precipitation (IPCC, 2007; Lau et al., 2006; Su et al., 2010; Johnson et al., 2004). The sources of atmospheric aerosols are primarily air pollution, fires, deserts and oceans.

Different modes of aerosol are characterized by different radiative properties. Ferrare et al. (2005) investigated the representation of the various types of aerosol (sulfate, black carbon, sea salt, particulate organic matter and dust) in various models and concluded that there are large differences in their properties, which may be the reason for inter-model and/or model-data differences and the consequent aerosol radiative effects. The same conclusion was made by Textor et al. (2006), who examined aerosol component life cycles for 17 aerosol modules of global models that participated in common experiments of the AeroCom initiative. Consequently, the international scientific community (IPCC, 2007) urged for a better understanding of the aerosol optical properties which are key parameters in determining their radiative effect/forcing (Hatzianastassiou et al., 2004).

The motivation for analysing aerosol optical depth (AOD) is that this is a good measure of atmospheric aerosol load and along with the two other aerosol optical properties, namely single scattering albedo (SSA) and asymmetry parameter (ASY), are all required to accurately determine aerosol radiative effects. The great advances in surface- and satellite-based monitoring instruments during the last decade have largely enhanced our ability to measure the atmospheric column aerosol load, and thus AOD, on a planetary scale. The combination of ground-based stations (e.g. AErosol RObotic NETwork, AERONET) and space-borne instruments, like MODIS (MOderate Resolution Imaging Spectroradiometer), MISR (Multi-angle Imaging SpectroRadiometer), TOMS (Total Ozone Mapping Spectrometer), AVHRR (Advanced Very High Resolution

ACPD
13, 5123–5163, 2013

Radiometer), provides a comprehensive map of the spatial and temporal distribution of AOD over most of the globe. There are numerous studies that have used either satellite products only or in combination with ground-based observations to estimate regional and global AOD (e.g. Papadimas et al., 2009; Levy et al., 2010). A synthesis of products from different satellite platforms should also improve estimates of AOD (Chatterjee et al., 2010).

All of the above-mentioned globally distributed satellite AOD products refer to columnar aerosol loads. Nevertheless, not only the horizontal but also the vertical distribution of aerosols is an important issue (Kaufman et al., 1997). Knowledge of the vertical structure of an aerosol layer is essential for modelling and understanding the processes involved (e.g. De Graaf et al., 2007) and specifically, for estimating the magnitude of the aerosol direct (Abel et al., 2005), indirect and semi-direct effects (Penner et al., 2006) at the boundaries of the atmosphere – top of atmosphere and Earth's surface – and within it. The vertical aerosol distribution is considered to be a great uncertainty (IPCC, 2007), therefore it has already been the subject of a number of studies (e.g. Liu et al., 2008; Yu et al., 2010). Most of them, though, focus on a limited number of sites, where ground-based remote sensing instruments (lidars) are available to provide vertical profiling of aerosols. Given that, as these studies verify, the vertical distribution of aerosols changes significantly from one site to another, obtaining a complete spatial picture of this distribution is of primary importance. Currently, such a global-scale picture is possible only based on models or recent satellite (CALIPSO, CloudSat) observations.

In order to derive characteristic aerosol properties on a global scale, complete and consistent fields – defined by AeroCom (Kinne et al., 2006) monthly median maps – have been improved with quality multi-annual monthly statistics by ground based sun-/sky-photometry (AERONET observations from 1998 to 2007) resulting in the Hamburg Aerosol Climatology (HAC). For a complete description of the algorithms and methodology used for the construction of the HAC, see Kinne et al. (2008, 2013). The main advantages of HAC are: (1) it provides aerosol optical properties for all sub-spectral regions of the solar and infrared spectrum, (2) it defines the vertical distribution of AOD

ACPD
13, 5123–5163, 2013

and (3) it separates optical properties for fine and coarse aerosols, as well as for pre-industrial and anthropogenic aerosol even as a function of time.

The purpose of this study is to assess the performance of HAC for use in climatological studies, by comparing it against contemporary and successfully validated satellite retrievals (Sect. 3). Although this has been shown indirectly in the past (Kinne et al., 2006) by assessing optical properties in 20 aerosol models participating in AeroCom and comparing them against remote sensing retrievals, the period of remote sensing data used there only covered one year (March 2000 to February 2001). As HAC intends to serve as a climatological dataset, it is important to compare it against satellite data from as many years as possible. Therefore, our MODIS data cover the period from March 2000 to February 2007 and CALIOP data are from July 2006 to January 2011. Furthermore, that study (Kinne et al., 2006) only presented mid-visible AOD, while this study also looks at the spectral performance of HAC AOD (Sect. 4). Finally, the vertical distribution of HAC is evaluated here, which is mostly based on HAM (Hamburg Aerosol Module) aerosol module within ECHAM general circulation model (Sect. 5). It would be also important to evaluate the HAC SSA and ASY data, but here priority is given to AOD, first because of its primary importance for the computation of aerosol radiative properties and climatic effects. In addition, presently there are enough available satellite and surface based AOD data for inter-comparison, which unfortunately is not the case, especially for SSA, but also for ASY.

2 Data

2.1 Hamburg Aerosol Climatology (HAC)

The new aerosol Climatology (HAC) provides all-sky aerosol optical properties for 14 solar and 16 infrared wavelengths, which complement the sub-spectral choices of radiative transfer models (RTM) and trace-gas absorption models. They are provided on a monthly basis and at $1^{\circ} \times 1^{\circ}$ latitude-longitude resolution over the globe

ACPD
13, 5123–5163, 2013

(ftp://ftp-projects.zmaw.de/aerocom/Climatology/2010/). They are given as total columnar values, but also for 20 pre-defined vertical levels extending from the surface to 20 km, thus providing a detailed vertical distribution. HAC also distinguishes aerosol optical properties of fine and coarse sizes. This distinction also includes separate definitions for aerosol altitude distributions based on simulations with HAM within ECHAM5 (Stier et al., 2007). In fact, HAC AOD is divided into anthropogenic ($AOD_{anthrop}$, the difference between current and pre-industrial fine aerosol) and natural ($AOD_{natural}$, the sum of pre-industrial fine aerosol and coarse aerosol) components. For AOD, the following mixing rule formulas are valid:

$$AOD_{total} = AOD_{fine} + AOD_{coarse} = AOD_{natural} + AOD_{anthrop} \quad (1)$$

Anthropogenic aerosols (Fig. 1b) dominate over heavily polluted areas, such as South-East Asia around Bejing (largest fine AOD values) or over northern India, East and Central Europe and Eastern United States. Also a fraction of AOD from wildfires is considered anthropogenic with major contributions over the Amazon basin (Holben et al., 1996; Fearnside, 2000) and western, central and southern Africa (Liousse et al., 1996; Swap et al., 1996; Johnson et al., 2008; Roberts et al., 2009). Anthropogenic AOD is mainly found over North Hemisphere land, but also over oceans due to transport from their sources. Averaging all grids across the globe and applying latitudinal weights, global anthropogenic AOD (at 550 nm wavelength) is found to be 0.037 (Table 1). The largest anthropogenic AOD occurs during NH summer and autumn (corresponding to1.14 and 1.05 times the mean annual global anthropogenic AOD). Natural aerosols are systematically found above deserts such as Sahara, Saudi Arabia, Gobi and Taklamakan deserts (Fig. 1c). Larger values of natural aerosol AOD also appear over southern oceans at latitudes between 45° S and 60° S, mainly sea salt type, as also reported by other studies (Chin et al., 2002; Penner et al., 2002). Some dust outflow from Patagonia is also evident at 40° W, in agreement with observations (Johnson et al., 2011). The global natural AOD (at 550 nm wavelength) is 0.093, which is almost three times larger than the global anthropogenic AOD (Table 1). Both the global

ACPD
13, 5123–5163, 2013

and seasonal distributions of natural AOD differ from distributions for anthropogenic aerosol. Natural AOD maxima in NH spring and summer are driven by dust contributions from northern Africa (e.g. de Meij and Lelieveld, 2011). Although wildfire burning also occurred at pre-industrial times, its AOD contributions to natural aerosol are limited.

Spectral and zonal variation of AOD (see Figs. S1 and S2 of Supplement, respectively) reproduces features like stronger variability of AOD with wavelength for anthropogenic than natural aerosol and clear inter-hemispherical asymmetry of AOD with larger values in NH than in SH. Nevertheless, this asymmetry is far stronger for anthropogenic (single peak near 30–50° N) than natural AOD, which apart from a primary peak in 10–30° N also exhibits a secondary peak in 45–55° S.

2.2 MODIS

HAC AOD is compared to monthly level 3 MODIS Collection 5 (C005) data from March 2000 to February 2007. The reason for using MODIS and not some other satellite platform is that MODIS products have been extensively validated and regarded as the most reliable global satellite AOD datasets to date, as shown by various validation studies against reference AERONET data (e.g. Levy et al., 2010; Remer et al., 2005; Ichoku et al., 2002; Chu et al., 2002). The Deep Blue MODIS datasets could also be potentially used, but due to their limited validation to date it has been decided not to be used in this study. MODIS sensors on the Terra and Aqua satellites retrieve during one overpass per day for each location aerosol products over land and ocean in a variety of spectral bands, from blue to thermal infra-red (Kaufman et al., 1997; Remer et al., 2005), every 1–2 days with a 16-day repeat cycle. The expected errors in MODIS derived AODs over land, based on overpass events over AERONET sites, are $\pm(0.05 + 0.20 \times \mathrm{AOD})$ for Collection 5 (Levy et al., 2010), whilst the pre-launch uncertainty of AOD over ocean is $\pm(0.05 + 0.05 \times \mathrm{AOD})$ (Remer et al., 2002).

Remote sensing of aerosol optical properties from a satellite highly depends on the wavelength of the reflected solar radiation and the reflectivity of the surface. Maximum

ACPD
13, 5123–5163, 2013

sensitivity to aerosol optical depth occurs over surfaces with low reflectance, such as ocean surfaces or dark land surfaces (King et al., 1999). On the other hand, for brighter surfaces, such as deserts and ice sheets, aerosol retrievals are more difficult, resulting in missing values for several months and for certain locations in MODIS C005. In presenting MODIS AOD data from several years there is a trade-off between the more appropriate temporal representation and the more appropriate spatial representation. We have chosen to use the following criterion in order to plot the maps that will be used for the comparison: for each season of each year at least 2 out of the months of the period should be available. Then for each year, the annual mean value has been calculated and presented only when all 4 seasons were available. Finally, for the mean values of all the period at least 3 out of 7 annual values were required. This strict criterion resulted in several missing grid cells (Fig. 2), especially during winter (DJF) when a large part of Northern Hemisphere land areas are covered by deserts (or clouds) and snow, making retrieval from MODIS impossible.

Levy et al. (2010) thoroughly assessed the performance of the aerosol products over dark-land targets by using a new algorithm. From their analysis, it was clear that the MODIS AOD retrieval often picks incorrect aerosol compositions, which in turn affects the accuracy of the retrieved AOD value. Thus, users of satellite data need to be cautious when using some of the products. Following their study, it has also been decided to permit negative AOD values down to −0.05, in order to reduce statistical biases in low AOD-conditions. Generally speaking, MODIS aerosol retrievals over oceans are more reliable than over land (Levy et al., 2010). Note that an important factor for MODIS erroneous or impossible retrievals – as well as for any other satellite- is cloud contamination. When the cloud fraction goes above 20 %, the mean MODIS overestimation approaches 0.03–0.04 or 15–20 %, additionally to the uncertainty that arises due to the type of surface (Levy et al., 2010).

ACPD
13, 5123–5163, 2013

2.3 CALIOP

The CALIPSO satellite was launched in April 2006 (Winker et al., 2007) with the main objective to provide the scientific community with global, day and night data of the vertical distribution of cloud and aerosol optical properties. The primary payload of the CALIPSO satellite is a two-wavelength and polarization-sensitive elastic backscatter lidar, the CALIOP instrument. An extensive discussion on the uncertainties in the CALIPSO calibration is found in Powell et al. (2009), and the conclusion is that calibration is expected to have a bias no larger than 5 %. Version 3.01 (released in May 2010) performs better than version 2 in daytime retrievals. Night-time performance is essentially the same, as night-time calibration procedures were unchanged in Version 3.01 (Rogers et al., 2011). In clear-sky conditions, Mona et al. (2009) found CALIOP to bias slightly low in the free troposphere and very low in the planetary boundary layer (PBL, below 2.5 km), probably due to erroneous cloud masking algorithms. However, Rogers et al. (2011) found good agreement between airborne and CALIOP 532 nm total attenuated backscatter inside the PBL (below ∼ 3 km). One of the weaknesses of CALIOP retrieval process is the misinterpretation of heavy aerosol loads as clouds (Pappalardo et al., 2010).

The CALIOP Version 3 data, which are used here as reference for the AOD vertical distribution, have matured through increasing validation to surface-based lidar measurements, e.g. EARLINET (European Aerosol Research Lidar Network) and NIES (National Institute for Environmental Studies). The data that we used here cover the period from July 2006 to January 2011. Vertical information has been assigned to 200 vertical layers of 100 m thickness each. The number of layers has been chosen accordingly, so that it matches the vertical layers provided by HAC. The vertical resolution of CALIOP varies according to the altitude, being 30 m between −0.5 km and ∼ 8.2 km and 60 m from ∼ 8.2 km to ∼ 20.2 km. In terms of data quality screening, one of the retrieval confidence measures is CAD (Cloud Aerosol Discrimination) score. In our study, we have used a threshold of CAD score smaller than 50, which keeps out most of

ACPD
13, 5123–5163, 2013

the dubious retrievals. CALIOP is a polar-orbiting satellite with a period of around 16 days. Therefore, the representation of its retrievals is not always ideal and CALIOP data retrievals need to be used with due care.

3 Evaluation of HAC aerosol optical depth (AOD)

3.1 Regional patterns

The comparison between HAC and MODIS AODs averaged on a global and hemispherical basis (Table 2) shows overall lower AOD values for HAC. The HAC mean annual global AOD value at 550 nm (corresponding global distribution shown in Fig. 1a) is 0.130, being smaller than MODIS (0.159, corresponding global distribution shown in Fig. S3, Supplement) by −18.2 %. Takemura et al. (2002) used a global three-dimensional model and found an annual global AOD equal to 0.116, while Ramanathan et al. (2001) found a value of 0.12±0.04. When averaging HAC on the basis of common pixels with MODIS, AOD slightly increases to 0.132 (Table 2), still lower than MODIS by −14.7 %. It should be noted that one of the reasons for higher values provided by satellite retrievals is undetected cloud contamination.

According to HAC, there is a strong inter-hemispherical asymmetry in terms of AOD, with the values for NH being almost double than that for SH (ratio equal to 1.68). Such a contrast is also found in MODIS with a ratio of 1.55. The relative annual hemispheric AOD difference between common HAC and MODIS pixels is slightly smaller for N. Hemisphere (−16.2 %) than for S. Hemisphere (−17.1 %). However, the larger MODIS AOD value (of 0.123 compared to 0.097 by HAC) for SH likely reflects a positive MODIS bias, due to poor cloud screening over the Southern Oceans.

In order to better assess the HAC-MODIS differences, the AOD values (at 550 nm) were also compared separately over land and over ocean. Our MODIS AOD over land value (0.209) agrees with the corresponding value provided by Levy et al. (2010). For the same period used in this study, Remer et al. (2008) found a global over land value of

ACPD
13, 5123–5163, 2013

0.19 in both Aqua and Terra. For the global land, including global deserts (not covered by MODIS here), Yu et al. (2006) refers to published Multi-angle Imaging SpectroRadiometer (MISR) data that yield a value of mean AOD of 0.23 ± 0.05. Note also that sampling frequency and hence reliability is larger with MODIS than with MISR. For the global ocean, the MODIS value is 0.149, close to those found in literature (e.g. 0.13–0.14 at Yu et al., 2006 and Remer et al., 2008). It appears that HAC AOD values (0.19 and 0.118 for land and ocean, respectively, Table 2) are closer to MODIS retrievals over land areas (bias equal to −9.1 %), which are more abundant in N. Hemisphere, while the agreement is not that good over oceanic areas (bias of −20.1 %), which are dominant in S. Hemisphere. However, there have been a lot of issues reported in the literature on the accuracy of MODIS retrievals (e.g. Papadimas et al., 2009; Levy et al., 2010; Zhang and Reid, 2010). Zhang and Reid (2010) have made an extensive study on the various versions of MODIS products and one of their findings was that the increased Level 3 AOD over Southern Ocean is mostly caused by cloud contamination. Based on that finding, the large disagreement between HAC and MODIS ocean/S. Hemisphere AOD is improved. In general, it has been shown in several studies that lower AOD values, i.e. over oceans, are biased high by MODIS, while the higher AOD values, over land, are biased low (Remer et al., 2005; Levy et al., 2005). Another issue in MODIS uncertainties is its overestimation in fine-mode aerosol sites by ~ 0.02 (Levy et al., 2010), which if taken into account can lead to a reduction in the N. Hemisphere HAC-MODIS difference (Table 2).

Since the accuracy of MODIS retrievals largely depends on the type of surface (Levy et al., 2010), a closer look into regional patterns would enable us to draw further conclusions on the accuracy of HAC AOD values, taking into consideration the possible errors in MODIS retrievals and discuss them in the context of the relevant literature. The study of Levy et al. (2010) was based on specific sites and not on whole regions, so the selection of the sites could cause biases with regards to the general trend for whole regions. However, due to the fact that there are certain areas with homogeneous profile of aerosol load, a projection from individual sites to larger areas could

ACPD
13, 5123–5163, 2013

be justified. At a first glance, it is clear that AOD differences are not systematic, but strongly depend on latitude and longitude, taking both positive and negative values (Fig. 2). HAC mainly overestimates AOD with respect to MODIS over land areas, by up to 0.2 (or 100 %), with some exceptions like western USA, Amazonian basin, central Africa or India where it underestimates AOD. The areas with larger HAC AOD are mostly areas with heavy aerosol load, either due to pollution (East Europe, East coast of United States), or due to desert dust (the coast off N. Africa, Gobi desert, the coast off West Africa), or due to biomass burning smoke (east coast of S. America and S. Africa). Note that MODIS tends to overestimate AOD over surfaces that are brighter and less green than optimal, like Central Africa or western USA (Levy et al., 2010). Furthermore, MODIS is shown previously to slightly overestimate compared to ground-based AERONET network by 0.05 or 60 % over areas with fine-aerosol, like eastern United States (Levy et al., 2010). HAC seems to suffer from a similar problem, based on the positive values over that area (Fig. 2, all plots). In general, HAC AOD values over oceans seem to be consistently lower than MODIS, having differences as large as about −60 %, especially in the tropics. However, during NH summer period and for the upper part of the southern windy zone, HAC reproduces higher AOD values by up to 70–80 %. This situation, which is also observed in NH spring but to a lesser extent, is reversed during NH autumn and winter, probably due to misclassification of sub-pixel clouds as coarse aerosol by MODIS. It is interesting to note that larger values of HAC are found over oceanic areas undergoing dust export, e.g. over the northern tropical Atlantic Ocean, where it is possible that MODIS tends to identify heavy dust events as clouds. In general, HAC seems to agree better with MODIS over land than ocean (especially in N. Hemisphere) verifying thus the conclusions drawn from the results of Table 2.

3.2 Seasonal patterns

On a global seasonal basis, the HAC-MODIS differences (Table 2) reveal a relatively weak annual cycle, reaching values of −20.1 % and −19.9 % in the NH autumn and

ACPD
13, 5123–5163, 2013

winter, and dropping down to −13.8 % in summer (JJA). The seasonal plots (Fig. 2a–d) show that there is non-uniform pattern over the Amazon basin. During NH summer, HAC AOD is larger than MODIS AOD in southern and eastern parts of Amazon basin, while the sign is opposite in northern and western parts of the basin. On the other hand, during NH spring, autumn and winter, HAC AOD is smaller than MODIS AOD over the largest part of the basin. It should be noted that MODIS might often misinterpret large biomass burning events as clouds and exclude them from the retrieval process, resulting in a better agreement during late NH summer and worse agreement in NH autumn. The missing grids in the region in NH spring and summer plots are most likely due to large cloud cover or zero values of MODIS that have been artificially excluded from the plots. Over North Australia, HAC AOD values are smaller/larger than MODIS in the dry/wet local season by up to more than 40 %.

The seasonal variation of global and hemispherical averages of HAC and MODIS AOD (Fig. 3a and Table 2) reveals that there is an almost similar inter-annual cycle. However, while for MODIS highest values appear during NH spring (0.168) and summer (0.167), for HAC NH spring values rise up to 0.137, while in summer (JJA) they peak at 0.144. Also, it appears that global HAC AOD values are systematically lower than MODIS ones throughout the year (Fig. 3b). The hemispherical AOD differences reveal that the largest global HAC-MODIS AOD differences arise from largest deviations in SH during local summer (DJF). The results of Fig. 3b prove that any assessment of AOD differences between the two databases has to be made rather separately on hemispherical or even better on a regional scale than on global, since the sign of the difference is mixed. Possible reasons for these differences could be biases of the model dependent background of the HAC involving model input (e.g. emissions, meteorology) and aerosol processing (e.g. transport and removal) or biases to assumptions for aerosol composition and environment in MODIS AOD retrievals.

The overall comparison between HAC and MODIS AOD is given in the scatterplots of Fig. 4, where monthly values for all grid cells at 1° latitude by 1° longitude resolution have been used. On an annual basis, there is a relatively good agreement between

ACPD
13, 5123–5163, 2013

the two datasets, yielding a correlation coefficient (R) equal to 0.76 for NH and 0.66 for SH and a RMSE of 0.072 and 0.043 for NH and SH, respectively. Seasonally, for NH, the worst fit, in terms of R-values, is found in boreal spring. Nevertheless, apart from lowest correlation coefficient ($R = 0.68$), the bias (−0.01) and RMSE (0.092) are the smallest, indicating a very good agreement. The best fit for NH is in winter, with the largest correlation coefficient ($R = 0.68$) and second smallest bias (−0.001) and RMSE (0.069). Taking into account all statistical parameters, for the SH, the worst fit is in boreal autumn ($R = 0.67$, bias = −0.041, RMSE = 0.07) and the best fit appears to be in NH summer ($R = 0.64$, bias = −0.001, RMSE = 0.06). The only positive bias (0.001) of HAC is found in summer (JJA) for SH, in agreement with the larger oceanic values mentioned earlier (Fig. 2). In terms of values of RMSE, the agreement between HAC and MODIS is better in light aerosol conditions, namely DJF for NH and JJA for SH and worse in heavy aerosol conditions (MAM for NH and SON for SH).

4 Spectral validation of AOD

Aerosol optical properties exhibit a significant variation with wavelength. Knowledge of aerosol optical properties on several wavelengths and for different parts of the electromagnetic spectrum can be of great use to identify different aerosol sizes and types (Vardavas and Taylor, 2011) and for efficiently estimating aerosol radiative and climatic effects (Hatzianastassiou et al., 2004). Radiative transfer and climate models need to cover the entire solar spectral range (extending at least up to 5000 nm) and beyond that up to the far infrared terrestrial spectrum in terms of aerosol, apart from others, optical properties. One of the great advantages of the new aerosol HAC is that it provides aerosol data with such a large spectral coverage. Here we attempt to maximize this advantage of HAC AOD, by evaluating its spectral AOD profiles. In order to do so, both HAC and MODIS AODs are compared against data from ground-based AERONET stations, usually considered as the truth amongst the aerosol community. It should be remembered that MODIS aerosol models are somehow tied to the adopted AERONET

ACPD
13, 5123–5163, 2013

ones ("Algorithm for Remote Sensing of Tropospheric Aerosol from MODIS", ATBD-MOD-02; http://modis.gsfc.nasa.gov/data/atbd/atmos_atbd.php) and are therefore not totally independent. HAC data are not totally independent either, since they rely on AERONET station statistics to modify the modelling background but cannot retain in this process local detail, which is tested here. AERONET data from 1998 to 2007 (from 2001 for Jabiru and 1999 for Tahiti) and for the months of January (April for Dalanzadgad) and July (September for Alta Floresta) have been used and certain representative grids have been selected that correspond to the specific main aerosol types existing in the Earth's atmosphere: (a) desert dust, (b) maritime, (c) biomass burning and (d) urban. The five (5) sites that were selected are seen in Fig. 5. Based on the availability of AERONET and MODIS data, the spectral comparison is necessarily restrained in the range from 300 nm to 700 nm for continental sites, and from 300 nm to 2500 nm for oceanic sites, for which spectral AOD data are available from all three databases.

The AERONET Goddard Space Flight Center (GSFC in Greenbelt, Maryland, USA) is a site located in a suburb of Washington DC with the urban aerosol type being dominant. In January (Fig. 6a-i), HAC $AOD_{550\,nm}$ (0.096) is equal to MODIS $AOD_{550\,nm}$, but larger than AERONET by 39 %. The spectral variation of both HAC and MODIS is in good agreement to AERONET except for UV. For the July plot (Fig. 6a-ii), HAC again captures the AERONET spectral variation quite well, having slightly larger AOD normalised AOD values in the UV and near-IR. The July value of HAC AOD at 550 nm is 0.308, 20 % smaller than AERONET and 27 % smaller than MODIS.

For Alta Floresta (in the Amazonian basin, Brazil), a rural site directly influenced by smoke produced by biomass burning during the fire season (from June to October), HAC $AOD_{550\,nm}$ is smaller than AERONET and MODIS by 22 % and 14 %, respectively, in January (Fig. 6b-i) and by 44 % and 50 %, respectively in September. HAC exhibits a stronger spectral decrease in the UV for both months which might be due to smaller particles assumed in HAC. MODIS spectral profile is identical to HAC during January and identical to AERONET during September.

ACPD
13, 5123–5163, 2013

Dalanzadgad is a small city (population is about 14 000) at an altitude of 1470 m in Central Asia, and more specifically in the Gobi desert in southern Mongolia. It is characterized by a typical cold desert climate with cold winters and hot summers. Here, the month of April has been used instead of January, as dust emission is at a maximum during April and spectral dependence is more important when AOD is high than when it is low. Note that for April (Fig. 6c-i) there are no MODIS data available over the area, possibly due to observational difficulties imposed by extended cloud coverage. Figure 8c reveals a stronger spectral dependence of HAC AOD than AERONET for the wavelengths smaller than 550 nm. For larger wavelengths, the spectral dependence is largely improved. Looking at the absolute values of AOD at 550 nm, both HAC and MODIS overestimate AOD compared to AERONET. This finding is in agreement with the study of Levy et al. (2010), who found that MODIS retrieval is biased high at this specific site. Eck et al. (2005) reported that AOD values remain relatively low all year with a monthly maximum of 0.20 in May and minimum of 0.05 to 0.06 (clean background levels) in December and January. HAC (and MODIS) overestimation, however, could be associated with the different spatial scales at which the spectral AOD data are reported in the three datasets and the strong spatial variability of AOD. Indeed, Kim et al. (2004) reported quite higher AOD values at Mandalgavi, which is also in Mongolia, about 275 km to north north-east of Dalanzadgad, with a long-term annual AOD mean of $\sim$ 0.4 at 500 nm, a value that is closer to that of HAC.

Jabiru is a site in North Australia (savanna), with complex aerosol composition consisting mainly of smoke from biomass burning and by maritime aerosols (Qin and Mitchell, 2009; Grey et al., 2006; Hyer et al., 2011). In January (Fig. 6d-i), HAC AOD exhibits a stronger spectral dependence than MODIS and AERONET. There is a much better agreement between HAC and AERONET in July. In terms of absolute values of AOD at 550 nm, HAC has smaller values than both AERONET and MODIS in January, but larger in July. Levy et al. (2010) had also found that MODIS retrieval is biased low in Jabiru.

ACPD
13, 5123–5163, 2013

Tahiti is an oceanic site, as it lies in the middle of the Pacific Ocean (Fig. 5). For sites over ocean, MODIS provides AOD for the wavelength spectrum from 470 to 2130 nm and AERONET from 340 to 1020 nm. The AOD values at this site are low, as expected in such clean maritime conditions (Smirnov et al., 2009). Sayer et al. (2010) reported measured AERONET AOD values ranging from 0.03 to 0.07 at 550 nm, in agreement with our HAC values. Although spectral dependence in UV wavelengths seems to be slightly stronger for HAC, the spectral profiles of all datasets seem to converge at larger wavelengths.

5 Vertical distribution of AOD

Vertical distribution of aerosols can yield variable results of radiative forcing and climate change, even if the columnar value of AOD or cloud amount is the same (Chung et al., 2010). In the present section we attempt first to get a global picture of the aerosol vertical distribution based on HAC, and then to evaluate this vertical distribution with CALIOP spaceborne lidar measurements. A detailed comparison between the HAC and CALIOP at global scale is beyond the scope of the present study; therefore we have chosen to perform a comparison only at the regional and local scales. Based on the required representativeness of the study region, we have selected to perform the comparison for the Mediterranean basin and for the specific world locations used in the previous section which are representative of various aerosol types. The Mediterranean basin has been selected as being a region with almost all types of aerosols coming from neighbouring natural and anthropogenic aerosol source areas, both continental and maritime (Lelieveld et al., 2002). Thus, local emissions along with small- and long-range transport processes are expected to shape different vertical aerosol distributions.

Figure 7 shows absolute HAC AOD values per layer of 1 km thickness each (top two rows) and the accumulated fraction of columnar AOD for fine, coarse and total aerosol for each altitude (bottom row). The computations/plots are made separately for 10-degree latitudinal zones of both hemispheres, as well as for the two hemispheres

ACPD
13, 5123–5163, 2013

and the globe, enabling us to get an overall global picture of the vertical distribution of aerosols. The zonal means indicate that the vertical distribution of aerosols is not the same for the two hemispheres. In N. Hemisphere the values of total (fine + coarse) AOD, i.e. the loadings of aerosols, for the lowest 5 km are about similar for the latitudes 0–60° N. Peaks are near 1.5–2.0 km and gradually decrease as we move from the equator to higher latitudes. Despite the fact that significant AOD values are found up to 5 km, most of the aerosol loading is confined in the boundary layer, i.e. up to 3–4 km. An interesting fact is that for the zone 70–90° N, a distinct amount of aerosol is found at altitudes between 10 and 20 km, i.e. in the polar stratosphere, with a peak at around 15 km (AOD values per km 0.0061–0.0146). Those values are in line with an observed/established (e.g. Matsui et al., 2011; Kondo et al., 2011) transport of aerosol from northern mid-latitudes towards the Arctic. Such distinct stratospheric aerosol amounts are not found in S. Hemisphere, specifically over southern polar latitudes. This is also verified by earlier (Stratospheric Aerosol Measurement – SAM2 – aboard Nimbus 7) or more recent satellite measurements (Stratospheric Aerosol Gas Experiment – SAGE-II, see http://data.giss.nasa.gov/cgi-bin/sageii/sageii_v6.cgi) revealing quite higher stratospheric aerosol extinction over northern than southern high latitudes, with maximum during NH spring and summer (Treffeisen et al., 2006). Instead, in S. Hemisphere, aerosols can be found above 10 km in the zones 50–70° S, though with smaller AOD values than in NH. The existence of aerosols in those high altitudes of SH seems to be consistent with the reported long-range, even semi-global, transport of aerosols, namely dust (Shaw, 1988), to the Antarctica's clean environment. As for the SH's troposphere, in general, aerosols are lifted up to slightly lower than NH's altitudes, i.e. up to about 3–4 km, confined in a shallower boundary layer due to the fact that SH is largely covered by oceans. Furthermore, according to HAC, the abundance of SH tropospheric aerosols is clearly reduced with respect to NH in all altitudes, with AOD not exceeding 0.028 per layer.

On a global basis, 50 % of the total AOD is found up to the height of 1.5 km (Fig. 7c-i) and 85 % of the total AOD is found from the surface up to 3.22 km above mean sea level

ACPD
13, 5123–5163, 2013

(a.m.s.l.) with corresponding heights (for 85 %) equal to 2.96 and 3.52 km for NH and SH, respectively. The vertical profiles of both fine and coarse aerosol are different for the two hemispheres, with fine aerosol being lifted a bit higher up into the atmosphere in S. than N. Hemisphere. Although the same is valid for coarse aerosols for latitudes up to 30° N and S, it is the opposite in higher latitudes (30–70°) where coarse aerosols are lifted higher up in S. than N. Hemisphere (right column).

Aerosol vertical profiles are highly dependent on season of the year (i.e. Vuolo et al., 2009) and on the site location characteristics (i.e. above desert or ocean or urban area). In order to visualize this, we produced the accumulated fractions of columnar AOD as functions of height, for total aerosol, for the Mediterranean basin (29.5–46.5° N, 10.5° W–36.5° E) for the months of January and July (Fig. 8a-i, a-ii). The profiles were produced using data from HAC and CALIOP. This comparison intends to provide researchers and potential users of HAC and CALIOP of the way aerosol is distributed vertically, regardless of the total columnar value. Nevertheless, note that differences already exist with regards to the latter. For instance, the mean HAC total columnar value for the entire Mediterranean region is 0.108 in January and 0.128 in July, while for CALIOP it is 0.083 and 0.172, respectively, indicating a stronger seasonality in the CALIOP data. For the same area, MODIS columnar AOD data exhibit a similar to CALIOP seasonality, though at higher values (0.116 and 0.238 for January and July, respectively). The comparison of vertical distribution of AOD reveals relatively small differences between HAC and CALIOP. In January 50 % (85 %) of columnar AOD in HAC is contributed by aerosols located below 1.2 km (2.1 km), when the same fraction of AOD in CALIOP is contributed by aerosols below 1.1 km (2.5 km). In July, the performance of HAC is even better. The largest difference occurs for the top 20 % of columnar AOD, where HAC places it above 1.9 km, while CALIOP detects it above 2.1 km. For both datasets, aerosols are dispersed vertically at higher altitudes in July than in January, due to the thicker warmer boundary layer, and HAC successfully captures this for the whole column.

ACPD
13, 5123–5163, 2013

At the GSFC site (Fig. 8b-i, b-ii), according to CALIOP retrievals, 50 % (85 %) of columnar aerosol is located below 800 m (1350 m) in January, while the same percentages for HAC are 1140 m (2100 m). A similar pattern, i.e. placement of less HAC AOD in lower altitudes, is found in the July plot of GSFC. The misplacement here is around 500 m for the bottom 50 % of AOD and decreases to 300 m for the bottom 85 % of columnar AOD.

The HAC-CALIOP comparison for the site of Alta Floresta (Fig. 8c-i, c-ii) is mixed. The July plot corresponding to high monthly AOD (due to biomass burning season) shows a very good agreement up to 2.2 km, while in the layers up to 5 km HAC places less aerosol than does CALIOP. The bottom 4 km-thick layer includes 97 % of HAC columnar AOD and 100 % of CALIOP columnar AOD. The January plot, on the other hand shows an identical vertical profile for both HAC and MODIS, with the main difference that HAC assumes a significantly smaller fraction of the columnar AOD at the boundary layer.

HAC and CALIOP profiles are quite different for January in Dalanzadgad (Fig. 8d-i, d-ii), with HAC having a smaller gradient of decreasing AOD, especially above 4.5 km, indicating non-negligible amount of aerosol above that altitude. For the July plot, there is very good agreement for the lowest 57 % of aerosol column load. Above that, HAC has a smoother curve, indicating small amounts of aerosol in the upper layers, in contrast to CALIOP that has a slightly sharper curve. Satheesh et al. (2009) reported that over India, 15–25 % of columnar AOD is contributed by aerosols below 1 km above ground. Bearing in mind that our altitudes are above mean sea level and the Dalanzadgad site is at 1470 m, the mentioned numbers are in good agreement with our study, despite the fact that HAC corresponds to a larger area.

A high bias of aerosol altitude by HAC is seen in the plots for Jabiru (biomass burning and maritime aerosol type; Fig. 10e-i, e-ii) and Tahiti (oceanic aerosol type; Fig. 10f-i, f-ii). In Jabiru, the difference for the bottom 50 % of columnar AOD is 1100 m (470 m) for January (July). For July, HAC assumes significantly more aerosol in the upper layers

ACPD
13, 5123–5163, 2013

(2–4 km), while CALIOP has detected practically all aerosols (95 %) up to the altitude of 1.94 km.

In Tahiti, there is again a misplacement of aerosols by HAC for both January and July, placing the top 55 % above 1.5–1.6 km, while CALIOP has detected only 4.2 % above that altitude. The vertical misplacement of aerosols from HAC ranges from ∼ 550 m for the bottom 10 % of columnar AOD to more than 1.1 km for the bottom 85 %.

6 Conclusions – discussion

The new Hamburg Aerosol Climatology (HAC) presented here is a mixture of ground-based AERONET observations and AeroCom model monthly mean fields. It has been shown to successfully reproduce well known geographical and temporal features of aerosol loading distributions. Furthermore, it seems to yield adequately patterns associated with global distributions of anthropogenic and natural aerosols, with estimated contributions to the global average total AOD by 28.5 and 71.5 %, respectively. For the annual anthropogenic load, the largest contribution is during NH summer and autumn by urban-industrial pollution. For the annual natural load, the largest contribution comes from NH summer and spring, most likely by desert dust and with some contribution from natural wildfires.

A comparison has been attempted against multi-annual aerosol data retrieved from contemporary satellite sensors, namely MODIS and CALIOP. The comparisons have been performed for the mid-visible (550 nm) aerosol optical depth (AOD), as this is the aerosol optical property quantifying the atmospheric aerosol loading, having large spatiotemporal variability, and always considered in radiative and climatic considerations with models. Comparing HAC with MODIS collection 5 data (from March 2000 to February 2008) at 1° × 1° (latitude/longitude) grid points, there were overall lower AOD values in the HAC. The HAC annual global mean total (natural plus anthropogenic) AOD is 0.132 whereas the annual global mean for MODIS is 0.159, thus larger by 0.027 or 17.0 %. Regionally, HAC has larger AOD values than MODIS in areas with

ACPD
13, 5123–5163, 2013

heavy aerosol load, mainly over land (namely northern subtropics), but smaller AOD than MODIS over ocean areas. An exception to that was the northern part of Southern Ocean, where HAC yields larger vales during NH spring and summer. HAC suggests 16.2 % lower AOD than MODIS for North Hemisphere and 17.1 % lower AOD for South Hemisphere. On a seasonal basis, HAC presents a summer (JJA) maximum (0.144), while MODIS maximum values are almost equal for spring (MAM) and summer (JJA), being 0.168 and 0.167, respectively. In terms of absolute and relative differences, the largest deviations occurred during months with heavy aerosol conditions, such as March to August for NH and from September to February for SH.

The spectral dependence of HAC AOD was also investigated by comparing it to MODIS and AERONET, yielding satisfactory results in most cases. For the examined sites and types of aerosol, HAC exhibits a stronger spectral dependence with wavelength for wavelengths between 300 and 550 nm. There is generally a better agreement between HAC and AERONET spectral dependence for larger wavelengths. This is true, even for sites with large values of AOD, such as Alta Floresta in September, which proves that HAC is successful in capturing the variation of AOD for a large part of the spectrum that is used in radiation transfer models.

The new HAC climatology provides a vertical profile of aerosols for the whole of the globe, which is valuable for radiative transfer and climate models, especially given that it is available separately for fine and coarse aerosols. The highest lifting of aerosols occurs in latitudes between the tropics and 30–40° N, and especially in the zone 20–30° N, reaching altitudes of 5–6 km. HAC also exhibits some aerosol over the Arctic, which is being transported from mid-latitudes. According to HAC, there are much less stratospheric aerosols over corresponding southern polar latitudes, though in South Hemisphere aerosols are found above 10 km in the zones of Southern Ocean (50–70° S), associated with coarse aerosols. The difference between the profiles of fine and coarse aerosol does not seem significant for either of the hemispheres, but in general fine aerosol is lifted higher up into the atmosphere than coarse aerosol in North Hemisphere, while the opposite is true for South Hemisphere. On a global basis, 50 %

ACPD
13, 5123–5163, 2013

of the total AOD is found up to the height of 1.5 km and 85 % of the total AOD is found from the surface up to 3.22 km above mean sea level. The corresponding fractions for the NH are 1.42 km and 2.96 km, whereas for SH are 1.70 and 3.52 km. HAC vertical distribution has been tested against Version 3 data from CALIOP from the period July 2006–January 2011. In the Mediterranean basin, HAC was found to have an almost perfect agreement for most of the tropospheric column. Looking at selected individual representative sites, and for the two months of January and July, we can conclude that HAC vertical distribution needs some tuning above areas with biomass burning smoke, desert dust and sea salt spray. The issue in some of those cases is that HAC assumes less aerosol in the lower layers (GSFC, January and July up to 2 km; Alta Floresta, from 2.2 to 6 km; Tahiti, January and July; Dalanzadgad, January and July up to 2 and 3 km; Jabiru, January and July), while in others more aerosol and larger fraction of columnar AOD is found at the lowest layers, compared to CALIOP (GSFC, January from 2 to 3 km and July from 3 to 9 km; Dalanzadgad, January up to 2 km and July above 2 km). The misplacement is usually smaller at the lower altitudes but increases as altitude increases, with a peak usually at 4–5 km.

According to our analysis, the HAC data for aerosol optical depth (AOD) have proven to be accurate enough to be used for aerosol studies, especially when it comes to locations, where neither ground-based or satellite data exist. They also offer great advantages consisting in the availability of vertically resolved AOD data, wide spectral coverage, as well as information on fine and coarse aerosols. The implementation of the HAC aerosol data, including single scattering albedo and asymmetry parameter, in a spectral radiation transfer model is the scope of ongoing work aiming at the quantification of anthropogenic/natural aerosol radiative forcings, and also at the assessment of the effect of the vertical misplacement of aerosols on the aerosol radiative effect.

Supplementary material related to this article is available online at: http://www.atmos-chem-phys-discuss.net/13/5123/2013/acpd-13-5123-2013-supplement.pdf.

ACPD
13, 5123–5163, 2013

Acknowledgements. The AeroCom (http://nansen.ipsl.jussieu.fr/AeroCom) global modelling effort was essential to this study, as the (16) model median provides the starting point for the new aerosol climatology (HAC). Thus the work of all global modelling groups that contributed to AeroCom is particular acknowledged. All AeroCom-based HAC data used here are freely available on the ftp site (ftp://ftp-projects.zmaw.de/aerocom/Climatology/2010/). The authors thank NASA-US for making available the Collection 005 Level-3 MODIS data. We thank the principal investigators and their staff for establishing and maintaining the 5 AErosol RObotic NETwork (AERONET) sites used in this investigation. We also thank CALIPSO Science Team for their efforts in making data products publicly available. CALIOP data were obtained from the NASA Langley Research Center Atmospheric Science Data Center.

References

Abel, S. J., Highwood, E. J., Haywood, J. M., and Stringer, M. A.: The direct radiative effect of biomass burning aerosols over southern Africa, Atmos. Chem. Phys., 5, 1999–2018, doi:10.5194/acp-5-1999-2005, 2005.

Balis, D., Papayannis, A., Galani, E., Marenco, F., Santacesaria, V., Hamonou, E., Chazette, P., Ziomas, I., and Zerefos, C.: Tropospheric LIDAR aerosol measurements and sun photometric observations at Thessaloniki, Greece, Atmos. Environ., 34, 925–932, 2000.

Chatterjee, A., Michalak, A. M., Kahn, R. A., Paradise, S. R., Braverman, A. J., and Miller, C. E.: A geostatistical data fusion technique for merging remote sensing and ground-based observations of aerosol optical thickness, J. Geophys. Res., 115, D20207, doi:10.1029/2009JD013765, 2010.

Chin, M., Ginoux, P., Kine, S., Torres, O., Holben, B. N., Duncan, B. N., Martin, R. V., Logan, J. A., Higurashi, A., and Nakajima, T.: Tropospheric aerosol optical thickness from the GOCART model and comparisons with satellite and Sun photometer measurements, J. Atmos. Sci., 59, 461–483, 2002.

Chu, D. A., Kaufman, Y. J., Ichoku, C., Remer, L. A., Tanre, D., and Holben, B. N.: Validation of MODIS aerosol optical depth retrieval over land, Geophys. Res. Lett., 29, 8007, doi:10.1029/2001GL013205, 2002.

Chung, C. E., Ramanathan, V., Carmichael, G., Kulkarni, S., Tang, Y., Adhikary, B., Leung, L. R., and Qian, Y.: Anthropogenic aerosol radiative forcing in Asia derived from regional mod-

ACPD
13, 5123–5163, 2013

els with atmospheric and aerosol data assimilation, Atmos. Chem. Phys., 10, 6007–6024, doi:10.5194/acp-10-6007-2010, 2010.
De Graaf, M., Stammes, P., and Aben, E. A. A.: Analysis of reflectance spectra of UV-absorbing aerosol scenes measured by SCIAMACHY, J. Geophys. Res., 112, D02206, doi:10.1029/2006JD007249, 2007.
De Meij, A. and Lelieveld, J.: Evaluating aerosol optical properties observed by ground-based and satellite remote sensing over the Mediterranean and the Middle East in 2006, Atmos. Res., 99, 415–433, 2011.
Eck, T. F., Holben, B. N., Dubovik, O., Smirnov, A., Goloub, P., Chen, H. B., Chatenet, B., Gomes, L., Zhang, X.-Y., Tsay, S. C., Ji, Q., Giles, D., and Slutsker, I.: Columnar aerosol optical properties at AERONET sites in central eastern Asia and aerosol transport to the tropical mid-Pacific, J. Geophys. Res., 110, D06202, doi:10.1029/2004JD005274, 2005.
Ferrare, R. A., Turner, D. D., Clayton, M., Guibert, S., Schulz, M., and Chin, M.: The vertical distribution of aerosols over the atmospheric radiation measurement Southern Great Plains Site, measured versus modelled, Fifteenth ARM Science Team Meeting Proceedings, Daytona Beach, Florida, March 14–18, 2005.
Forster, P., Ramaswamy, V., Artaxo, P., Berntsen, T., Betts, R., Fahey, D. W., Haywood J., Lean, J., Lowe, D. C., Myhre, G., Nganga, J., Prinn, R., Raga, G., Schulz, M., and Van Dorland, R.: Changes in atmospheric constituents and in radiative forcing, in Climate Change 2007: The Physical Science Basis – Contribution of Working Group I to the Fourth Assessment Report of the Intergovernmental Panel on Climate Change, edited by: Solomon, S., Qin, D., Manning, M., Chen, Z., Marquis, M., Averyt, K. B., Tignor, M., and Miller, H. L., 289–348, Cambridge Univ. Press, New York, USA, 2007.
Grey, W. M. F., North, P. R. J., Los, S. O., and Mitchell, R. M.: Aerosol optical depth and land surface reflectance from multiangle AATSR measurements: global validation and intersensor comparisons, IEEE T. Geosci. Remote, 44, 2184–2197, 2006.
Hatzianastassiou, N., Katsoulis, B., and Vardavas, I.: Global distribution of aerosol direct radiative forcing in the ultraviolet and visible arising under clear skies, Tellus B, 56, 51–71, 2004.
Holben, B. N., Setzer, A., Eck, T. F., Pereira, A., and Slutsker, I.: Effect of dry-season biomass burning on Amazon basin aerosol concentrations and optical properties, 1992–1994, J. Geophys. Res., 101, 19465–19481, doi:10.1029/96JD01114, 1996.

ACPD
13, 5123–5163, 2013

Hyer, E. J., Reid, J. S., and Zhang, J.: An over-land aerosol optical depth data set for data assimilation by filtering, correction, and aggregation of MODIS Collection 5 optical depth retrievals, Atmos. Meas. Tech., 4, 379–408, doi:10.5194/amt-4-379-2011, 2011.

Ichoku, C., Chu, D. A., Mattoo, S., Kaufman, Y. J., Remer, L. A., Tanré, D., Slutsker, I., and Holben, B. N.: A spatio-temporal approach for global validation and analysis of MODIS aerosol-products, Geophys. Res. Lett., 29, 8006, doi:10.1029/2001GL013206, 2002.

Johnson, B. T., Shine, K. P., and Forster, P. M.: The semi-direct aerosol effect: impact of absorbing aerosols on marine stratocumulus, Q. J. Roy. Meteorol. Soc., 130, 1407–1422, 2004.

Johnson, B. T., Osborne, S. R., Haywood, J. M., and Harrison, M. A. J.: Aircraft measurements of biomass burning aerosol over West Africa during DABEX, J. Geophys. Res., 113, D00C06, doi:10.1029/2007JD009451, 2008.

Johnson, M. S., Meskhidze, N., Kiliyanpilakkil, V. P., and Gassó, S.: Understanding the transport of Patagonian dust and its influence on marine biological activity in the South Atlantic Ocean, Atmos. Chem. Phys., 11, 2487–2502, doi:10.5194/acp-11-2487-2011, 2011.

Kaufman, Y. J., Tanre, D., Gordon, H. R., Nakajima, T., Lenoble, J., Frouin, R., Grassl, H., Herman, B. M., King, M. D., and Teilet, P. M.: Passive remote sensing of tropospheric aerosol and atmospheric correction for the aerosol effect, J. Geophys. Res., 102, 16815–16830, 1997.

Kim, D. H., Sohn, B. J., Nakajima, T., Takamura, T., Takemura, T., Choi, B. C., and Yoon, S. C.: Aerosol optical properties over East Asia determined from ground-based sky radiation measurements, J. Geophys. Res., 109, D02209, doi:10.1029/2003JD003387, 2004

King, M. D., Kaufmann, Y. J., Tanré, D., and Nakajima, T.: Remote sensing of tropospheric aerosols from space: past, present and future, B. Am. Meteorol. Soc., 80, 2229–2259, 1999.

Kinne, S.: Climatologies of cloud related aerosols – part 1 particle number and size, in: Clouds in the Perturbed Climate System, edited by: Heintzenberg, J. and Charlson, J., Cambridge, Mass.: MIT Press, 2008.

Kinne, S., Schulz, M., Textor, C., Guibert, S., Balkanski, Y., Bauer, S. E., Berntsen, T., Berglen, T. F., Boucher, O., Chin, M., Collins, W., Dentener, F., Diehl, T., Easter, R., Feichter, J., Fillmore, D., Ghan, S., Ginoux, P., Gong, S., Grini, A., Hendricks, J., Herzog, M., Horowitz, L., Isaksen, I., Iversen, T., Kirkevåg, A., Kloster, S., Koch, D., Kristjansson, J. E., Krol, M., Lauer, A., Lamarque, J. F., Lesins, G., Liu, X., Lohmann, U., Montanaro, V., Myhre, G., Penner, J., Pitari, G., Reddy, S., Seland, O., Stier, P., Takemura, T., and Tie, X.:

ACPD
13, 5123–5163, 2013

An AeroCom initial assessment – optical properties in aerosol component modules of global models, Atmos. Chem. Phys., 6, 1815–1834, doi:10.5194/acp-6-1815-2006, 2006.
Kinne, S., O'Donnel, D., Stier, P., Kloster, S., Zhang, K., Schmidt, H., Rast, S., Giorgetta, M., Eck, T., and Stevens, B.: A new global aerosol climatology for climate studies, Atmos. Chem. Phys. Discuss., in review, 2013.
Kondo, Y., Matsui, H., Moteki, N., Sahu, L., Takegawa, N., Kajino, M., Zhao, Y., Cubison, M. J., Jimenez, J. L., Vay, S., Diskin, G. S., Anderson, B., Wisthaler, A., Mikoviny, T., Fuelberg, H. E., Blake, D. R., Huey, G., Weinheimer, A. J., Knapp, D. J., and Brune, W. H.: Emissions of black carbon, organic, and inorganic aerosols from biomass burning in North America and Asia in 2008, J. Geophys. Res., 116, D08204, doi:10.1029/2010JD015152, 2011.
Lau, K. M., Kim, M. K., and Kim, K. M.: Asian summer monsoon anomalies induced by aerosol direct forcing: the role of the Tibetan Plateau, Clim. Dynam., 26, 855–864, doi:10.1007/s00382-006-0114-z, 2006.
Lelieveld, J., Berresheim, H., Borrmann, S., Crutzen, P. J., Dentener, F. J., Fischer, H. Feichter, J., Flatau, P. J., Heland, J., Holzinger, R., Korrmann, R., Lawrence, M. G., Levin, Z., Markowicz, K. M., Mihalopoulos, N., Minikin, A., Ramanathan, V., de Reus, M., Roelofs, G. J., Scheeren, H. A., Sciare, J., Schlager, H., Schultz, M., Siegmund, P., Steil, B., Stephanou, E. G., Stier, P., Traub, M.,Warneke, C., Williams, J., and Ziereis, H.: Global air pollution crossroads over the Mediterranean, Science, 298, 794–799, 2002.
Levy, R. C., Remer, L. A., Martins, J. V., Kaufman, Y. J., Plana-Fattori, A., Redemann, J., and Wenny, B.: Evaluation of the MODIS aerosol retrievals over ocean and land during CLAMS, J. Atmos. Sci., 62, 974–992, 2005.
Levy, R. C., Remer, L. A., Kleidman, R. G., Mattoo, S., Ichoku, C., Kahn, R., and Eck, T. F.: Global evaluation of the Collection 5 MODIS dark-target aerosol products over land, Atmos. Chem. Phys., 10, 10399–10420, doi:10.5194/acp-10-10399-2010, 2010.
Liousse, C., Penner, J. E., Chuang, C., Walton, J. J., Eddleman, H., and Cachier, H.: A global three-dimensional model study of carbonaceous aerosols, J. Geophys. Res., 101, 19411–19432, doi:10.1029/95JD03426, 1996.
Liu, D., Wang, Z., Liu, Z., Winker, D., and Trepte, C.: A height resolved global view of dust aerosols from the first year CALIPSO lidar measurements, J. Geophys. Res., 113, D16214, doi:10.1029/2007JD009776, 2008.
Matsui, H., Kondo, Y., Moteki, N., Takegawa, N., Sahu, L. K., Zhao, Y., Fuelberg, H. E., Sessions, W. R., Diskin, G., Blake, D. R., Wisthaler, A., and Koike, M.: Seasonal variation of the

ACPD
13, 5123–5163, 2013

transport of black carbon aerosol from the Asian continent to the Arctic during the ARCTAS aircraft campaign, J. Geophys. Res., 116, D05202, doi:10.1029/2010JD015067, 2011.
McCormick, M. P. and Brandl, D.: SAM II measurements of the polar stratospheric aerosol, NASA Reference Publication 1164, vol. VII, 1986.
Mona, L., Pappalardo, G., Amodeo, A., D'Amico, G., Madonna, F., Boselli, A., Giunta, A., Russo, F., and Cuomo, V.: One year of CNR-IMAA multi-wavelength Raman lidar measurements in coincidence with CALIPSO overpasses: Level 1 products comparison, Atmos. Chem. Phys., 9, 7213–7228, doi:10.5194/acp-9-7213-2009, 2009.
Papadimas, C. D., Hatzianastassiou, N., Mihalopoulos, N., Kanakidou, M., Katsoulis, B. D., and Vardavas, I.: Assessment of the MODIS Collections C005 and C004 aerosol optical depth products over the Mediterranean basin, Atmos. Chem. Phys., 9, 2987–2999, doi:10.5194/acp-9-2987-2009, 2009.
Pappalardo, G., Wandinger, U., Mona, L., Hiebsch, A., Mattis, I., Amodeo, A., Ansmann, A., Seifert, P., Linné, H., Apituley, A., Alados Arboledas, L., Balis, D., Chaikovsky, A., D'Amico, G., De Tomasi, F., Freudenthaler, V., Giannakaki, E., Giunta, A., Grigorov, I., Iarlori, M., Madonna, F., Mamouri, R.-E., Nasti, L., Papayannis, A., Pietruczuk, A., Pujadas, M., Rizi, V., Rocadenbosch, F., Russo, F., Schnell, F., Spinelli, N., Wang, X., and Wiegner, M.: EARLINET correlative measurements for CALIPSO: first intercomparison results, J. Geophys. Res., 115, D00H19, doi:10.1029/2009JD012147, 2010.
Penner, J. E., Quaas, J., Storelvmo, T., Takemura, T., Boucher, O., Guo, H., Kirkevåg, A., Kristjánsson, J. E., and Seland, Ø.: Model intercomparison of indirect aerosol effects, Atmos. Chem. Phys., 6, 3391–3405, doi:10.5194/acp-6-3391-2006, 2006.
Powell, K. A., Hostetler, C. A., Liu, Z. Y., Vaughan, M. A., Kuehn, R. E., Hunt, W. H., Lee, K. P., Trepte, C. R., Rogers, R. R., Young, S. A., and Winker, D. M.: CALIPSO Lidar calibration algorithms. Part I: Night-time 532-nm parallel channel and 532-nm perpendicular channel, J. Atmos. Ocean. Tech., 26, 2015–2033, 2009.
Qin, Y. and Mitchell, R. M.: Characterisation of episodic aerosol types over the Australian continent, Atmos. Chem. Phys., 9, 1943–1956, doi:10.5194/acp-9-1943-2009, 2009.
Ramanathan, V., Crutzen, P. J., Kiehl, J. T., and Rosenfeld, D.: Aerosols, climate, and the hydrological cycle, Science, 294, 2119–2124, 2001.
Remer, L. A., Tanré, D., Kaufman, Y. J., Ichoku, C., Mattoo, S., Levy, R., Chu, D. A., Holben, B., Dubovik, O., Smirnov, A., Martins, J. V., Li, R.-R., and Ahman, Z.: Validation of MODIS

ACPD
13, 5123–5163, 2013

aerosol retrieval over ocean, Geophys. Res. Lett., 29, 8008, doi:10.1029/2001GL013204, 2002.
Remer, L. A., Kaufman, Y. J., Tanre, D., Mattoo, S., Chu, D. A., Martins, J. V., Li, R. R., Ichoku, C., Levy, R. C., Kleidman, R. G., Eck, T. F., Vermote, E., and Holben, B. N.: The MODIS aerosol algorithm, products, and validation, J. Atmos. Sci., 62, 947–973, 2005.
Remer, L. A., Kleidman, R. G., Levy, R. C., Kaufman, Y. J., Tanre, D., Mattoo, S., Martins, J. V., Ichoku, C., Koren, I., Yu, H. B., and Holben, B. N.: Global aerosol climatology from the MODIS satellite sensors, J. Geophys. Res., 113, D14S07, doi:10.1029/2007JD009661, 2008.
Roberts, G., Wooster, M. J., and Lagoudakis, E.: Annual and diurnal african biomass burning temporal dynamics, Biogeosciences, 6, 849–866, doi:10.5194/bg-6-849-2009, 2009.
Rogers, R. R., Hostetler, C. A., Hair, J. W., Ferrare, R. A., Liu, Z., Obland, M. D., Harper, D. B., Cook, A. L., Powell, K. A., Vaughan, M. A., and Winker, D. M.: Assessment of the CALIPSO Lidar 532 nm attenuated backscatter calibration using the NASA LaRC airborne High Spectral Resolution Lidar, Atmos. Chem. Phys., 11, 1295–1311, doi:10.5194/acp-11-1295-2011, 2011.
Satheesh, S. K., Vinoj, V., Suresh Babu, S., Krishna Moorthy, K., and Nair, Vijayakumar S.: Vertical distribution of aerosols over the east coast of India inferred from airborne LIDAR measurements, Ann. Geophys., 27, 4157–4169, doi:10.5194/angeo-27-4157-2009, 2009.
Sayer, A. M., Thomas, G. E., and Grainger, R. G.: A sea surface reflectance model for (A)ATSR, and application to aerosol retrievals, Atmos. Meas. Tech., 3, 813–838, doi:10.5194/amt-3-813-2010, 2010.
Schulz, M., Textor, C., Kinne, S., Balkanski, Y., Bauer, S., Berntsen, T., Berglen, T., Boucher, O., Dentener, F., Guibert, S., Isaksen, I. S. A., Iversen, T., Koch, D., Kirkevåg, A., Liu, X., Montanaro, V., Myhre, G., Penner, J. E., Pitari, G., Reddy, S., Seland, Ø., Stier, P., and Takemura, T.: Radiative forcing by aerosols as derived from the AeroCom present-day and pre-industrial simulations, Atmos. Chem. Phys., 6, 5225–5246, doi:10.5194/acp-6-5225-2006, 2006.
Shaw, G. E.: Antarctic aerosols: a review, Rev. Geophys., 26, 89–112, 1988.
Smirnov, A., Holben, B. N., Slutsker, I., Giles, D. M., McClain, C. R., Eck, T. F., Sakerin, S. M., Macke, A., Croot, P., Zibordi, G., Quinn, P. K., Sciare, J., Kinne, S., Harvey, M., Smyth, T. J., Piketh, S., Zielinski, T., Proshuninsky, A., Goes, J. I., Nelson, N. B., Larouche, P., Radionov, V. F., Goloub, P., Moorthy, K. K., Matarresse, R., Robertson, E. J., and Jourdin, F.: Maritime Aerosol Network as a component of Aerosol Robotic Network, J. Geophys. Res., 112, D06204, doi:10.1029/2008JD011257, 2009.

ACPD
13, 5123–5163, 2013

Stier, P., Seinfeld, J. H., Kinne, S., and Boucher, O.: Aerosol absorption and radiative forcing, Atmos. Chem. Phys., 7, 5237–5261, doi:10.5194/acp-7-5237-2007, 2007.
Su, W., Loeb, N. G., Xu, K.-M., Schuster, G. L., and Eitzen, Z. A.: An estimate of aerosol indirect effect from satellite measurements with concurrent meteorological analysis, J. Geophys. Res., 115, D18219, doi:10.1029/2010JD013948, 2010.
Swap, R. J., Garstang, M., Macko, S. A., Tyson, P. D., Maenhaut, W., Artaxo, P., Kallberg, P., and Talbot, R.: The long-range transport of southern African aerosol to the tropical South Atlantic, J. Geophys. Res., 101, 23777–23791, doi:10.1029/95JD01049, 1996.
Takemura, T., Nakajima, H. T., Dubovik, O., Holben, B. N., and Kinne, S.: Single-scattering albedo and radiative forcing of various aerosol species with a global three-dimensional model, J. Climate, 15, 333–352, 2002.
Textor, C., Schulz, M., Guibert, S., Kinne, S., Balkanski, Y., Bauer, S., Berntsen, T., Berglen, T., Boucher, O., Chin, M., Dentener, F., Diehl, T., Easter, R., Feichter, H., Fillmore, D., Ghan, S., Ginoux, P., Gong, S., Grini, A., Hendricks, J., Horowitz, L., Huang, P., Isaksen, I., Iversen, I., Kloster, S., Koch, D., Kirkevåg, A., Kristjansson, J. E., Krol, M., Lauer, A., Lamarque, J. F., Liu, X., Montanaro, V., Myhre, G., Penner, J., Pitari, G., Reddy, S., Seland, Ø., Stier, P., Takemura, T., and Tie, X.: Analysis and quantification of the diversities of aerosol life cycles within AeroCom, Atmos. Chem. Phys., 6, 1777–1813, doi:10.5194/acp-6-1777-2006, 2006.
Treffeisen, R. E., Thomason, L. W., Ström, J., Herber, A. B., Burton, S. P., and Yamanouchi, T.: Stratospheric Aerosol and Gas Experiment (SAGE) II and III aerosol extinction measurements in the Arctic middle and upper troposphere, J. Geophys. Res., 111, D17203, doi:10.1029/2005JD006271, 2006.
Vardavas, I. M. and Taylor, F. W.: Radiation and Climate: Atmospheric energy budget from satellite remote sensing, International Series of Monographs on Physics No. 138, Oxford University Press, Oxford, 2011.
Vuolo, M. R., Chepfer, H., Menut, L., and Cesana, G.: Comparison of mineral dust layers vertical structures modeled with CHIMERE-DUST and observed with the CALIOP lidar, J. Geophys. Res.-Atmos., 114, D09214, doi:10.1029/2008JD011219, 2009.
Winker, D. M., Hunt, W. H., and McGill, M. J.: Initial performance assessment of CALIOP, Geophys. Res. Lett., 34, doi:10.1029/2007GL030135, 2007.
Yu, H., Kaufman, Y. J., Chin, M., Feingold, G., Remer, L. A., Anderson, T. L., Balkanski, Y., Bellouin, N., Boucher, O., Christopher, S., DeCola, P., Kahn, R., Koch, D., Loeb, N., Reddy, M. S., Schulz, M., Takemura, T., and Zhou, M.: A review of measurement-based assessments of the

ACPD
13, 5123–5163, 2013

aerosol direct radiative effect and forcing, Atmos. Chem. Phys., 6, 613–666, doi:10.5194/acp-6-613-2006, 2006.

Yu, H., Chin, M., Winker, D. M., Omar, A. H., Liu, Z., Kittaka, C., and Diehl, T.: Global view of aerosol vertical distributions from CALIPSO lidar measurements and GOCART simulations: Regional and seasonal variations, J. Geophys. Res., 115, D00H30, doi:10.1029/2009JD013364, 2010.

Zhang, J. and Reid, J. S.: A decadal regional and global trend analysis of the aerosol optical depth using a data-assimilation grade over-water MODIS and Level 2 MISR aerosol products, Atmos. Chem. Phys., 10, 10949–10963, doi:10.5194/acp-10-10949-2010, 2010.

ACPD
13, 5123–5163, 2013

Table 1. Annual and seasonal Hamburg Aerosol Climatology (HAC) global (no missing grids) values for total, anthropogenic and natural aerosol optical depth (AOD) at 550 nm.

	DJF	MAM	JJA	SON	annual
Anthrop. AOD	0.031	0.036	0.042	0.039	0.037
Natural AOD (pre-ind fine + coarse)	0.085	0.101	0.102	0.084	0.093
Fine AOD (pre-ind fine + anthrop.)	0.053	0.059	0.070	0.063	0.061
Coarse AOD	0.0635	0.078	0.074	0.060	0.069
Pre-ind. fine AOD	0.0215	0.023	0.028	0.024	0.024

ACPD
13, 5123–5163, 2013

Table 2. Total mid-visible (550 nm) Aerosol Optical Depth (AOD) for HAC and MODIS, and their absolute and relative [(HAC – MODIS)/MODIS] differences. Values are averaged over the globe and the two hemispheres, as well as over land and oceans separately. The values in brackets are for common HAC-MODIS pixels.

Aerosol Optical Depth (550 nm)	HAC	MODIS	HAC-MODIS	(HAC – MODIS)/MODIS (%)
Annual global	0.130 (0.132)	0.159	−0.029 (−0.027)	−18.2 (−17.0)
Annual N. Hemisphere	0.163 (0.160)	0.191	−0.028 (−0.031)	−14.7 (−16.2)
Annual S. Hemisphere	0.097 (0.102)	0.123	−0.026 (−0.021)	−21.1 (−17.1)
Land areas only (common pixels)	(0.190)	0.209	−0.019	−9.1
Ocean areas only (common pixels)	(0.118)	0.149	−0.031	−20.1
Winter	0.117 (0.121)	0.146	−0.029 (−0.025)	−19.9 (−17.1)
Spring	0.137 (0.137)	0.168	−0.031 (−0.031)	−18.5 (−18.5)
Summer	0.144 (0.145)	0.167	−0.023 (−0.022)	−13.8 (−13.2)
Autumn	0.123 (0.124)	0.154	−0.031 (−0.030)	−20.1 (−19.5)

ACPD
13, 5123–5163, 2013

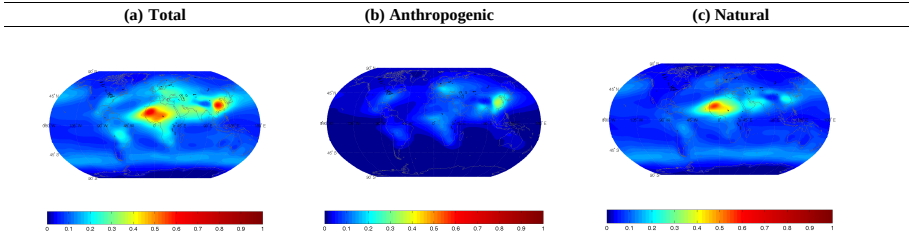

Fig. 1. Hamburg Aerosol Climatology (HAC) global annual distribution of aerosol optical depth at 550 nm. Results are given for **(a)** total, **(b)** anthropogenic (consisting of fine mode only), and **(c)** natural (pre-industrial-fine mode + coarse) aerosol.

ACPD
13, 5123–5163, 2013

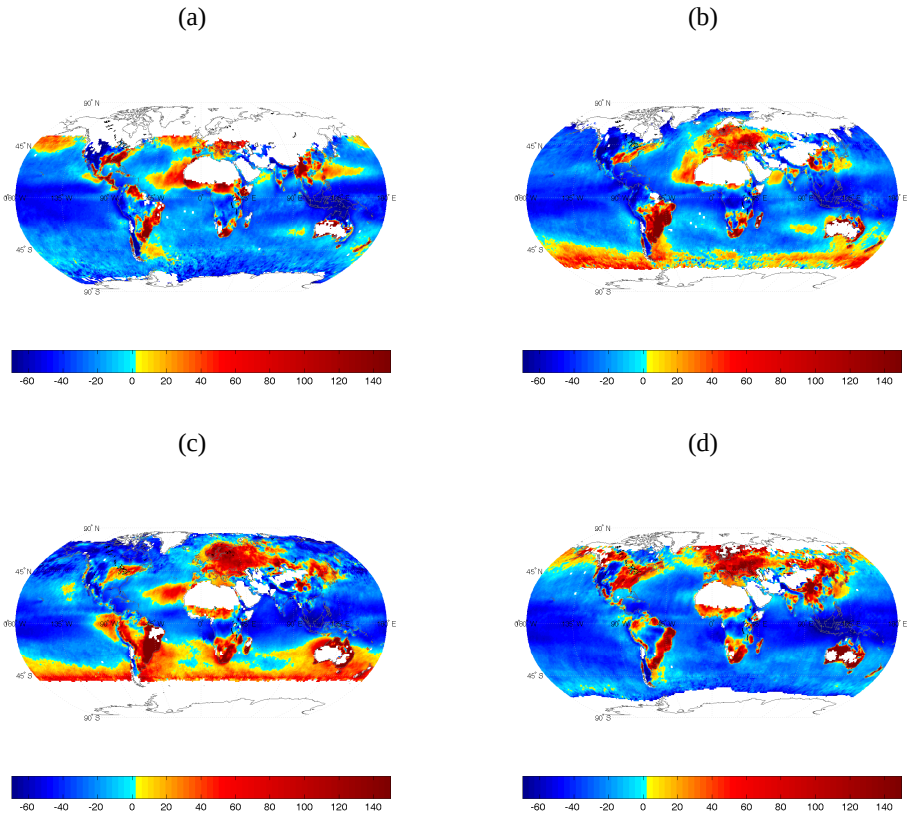

Fig. 2. Comparison between HAC and MODIS total aerosol optical depth at 550 nm. Global seasonal distribution of relative percentage differences ((HAC – MODIS)/MODIS – %) for: **(a)** winter (December-January-February), **(b)** spring (March-April-May), **(c)** summer (June-July-August) and **(d)** autumn (September-October-November). White shaded areas correspond to cases for which MODIS AOD values are missing or do not qualify for the averaging threshold.

ACPD
13, 5123–5163, 2013

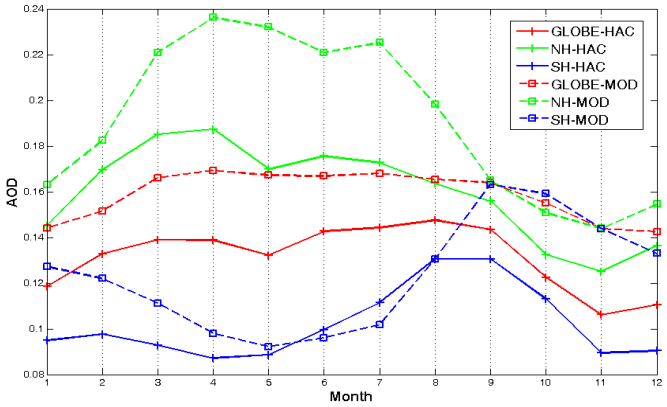

(a)

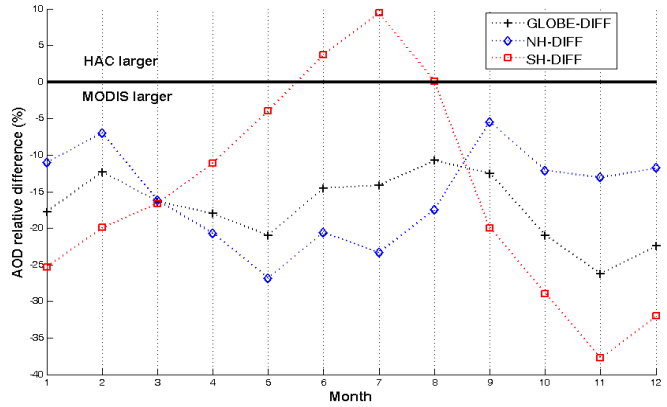

(b)

Fig. 3. Intra-annual variation of: **(a)** HAC (AeroCom based) and MODIS global and hemispherical monthly AOD and **(b)** HAC and MODIS global and hemispherical monthly AOD relative differences ([HAC – MODIS]/MODIS). Note the negative scale on y-axis in **(b)**. Values are for common grids.

ACPD
13, 5123–5163, 2013

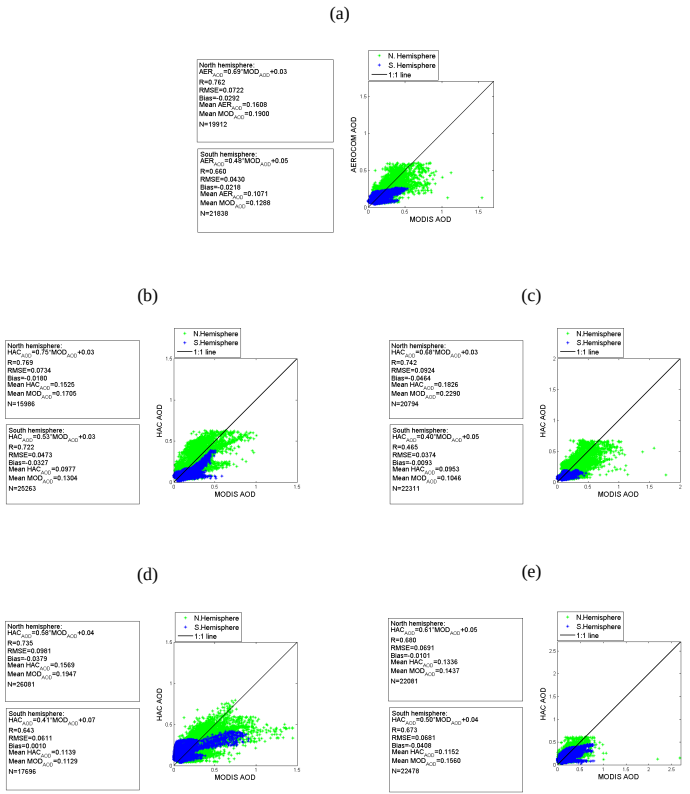

Fig. 4. Scatterplot comparison between total aerosol optical depth from HAC (AeroCom based) and MODIS datasets, for all months **(a)**, and for winter **(b)**, spring **(c)**, summer **(d)** and autumn **(e)**. Green points are for N. Hemisphere and blue points for S. Hemisphere. Black line in the plots is the 1 : 1 line. Statistics given in the textboxes in the plots separately for N. and S. Hemisphere are: the correlation coefficients (R), the root mean squared errors (RMSE), the mean values (Mean), and the number of matched data pairs (N).

ACPD
13, 5123–5163, 2013

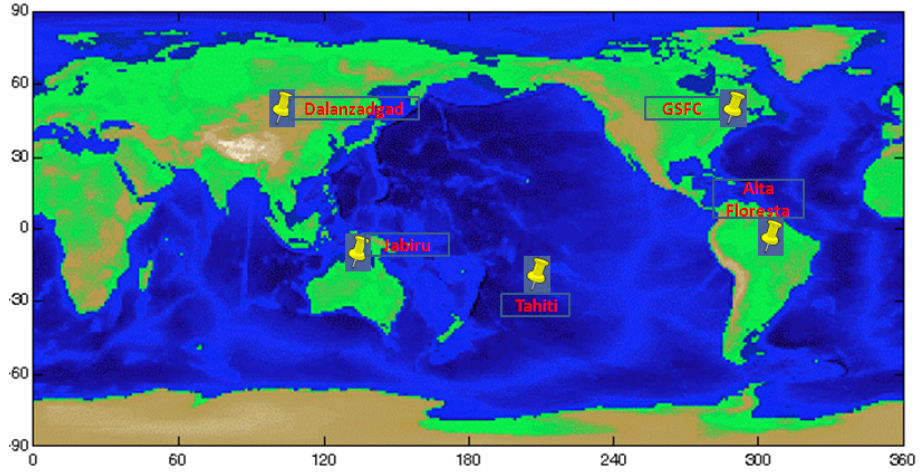

Fig. 5. World map with the five selected representative sites for which the spectral evaluation of AeroCom AOD is attempted. **(a)** GSFC (1998–2007, 38.99° North, 76.83° West), **(b)** Alta Floresta (1999–2007, 9.87° South, 56.10° West), **(c)** Dalanzadgad (1998–2007, 43.57° North, 104.41° East), **(d)** Jabiru (2000–2007, 12.66° South, 132.89° East) and **(e)** Tahiti (1999–2007, 17.57° South, 149.60° West).

ACPD
13, 5123–5163, 2013

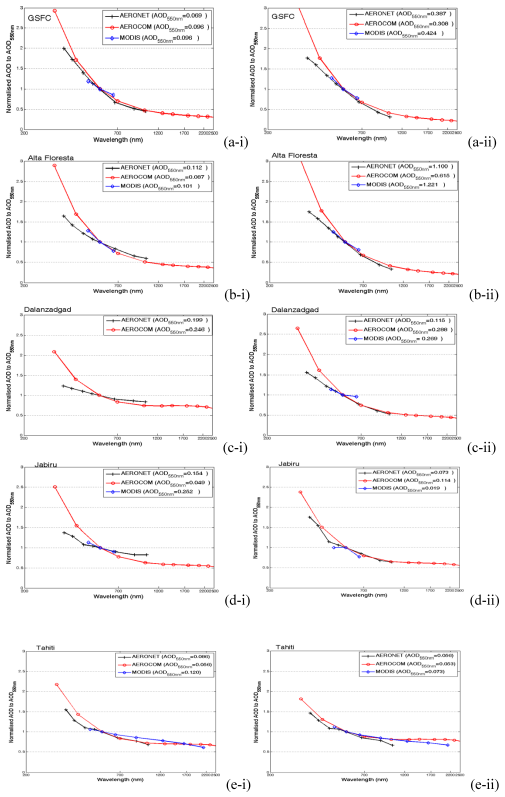

Fig. 6. Spectral profile of Aerosol Optical Depth (AOD) and the differences between the three datasets over the five selected sites (see Fig. 5) for January (left column, all sites except Dalanzadgad where April is shown) and July (right, all sites except Alta Floresta, where September is shown). Symbols and lines are: solid black lines with plus signs for AERONET data, solid red lines with circles for HAC data, solid blue lines with diamonds for MODIS. The values on y-axes are AOD values normalised to the AOD value at 550 nm. The legend boxes mention AOD for each dataset at 550 nm.

ACPD
13, 5123–5163, 2013

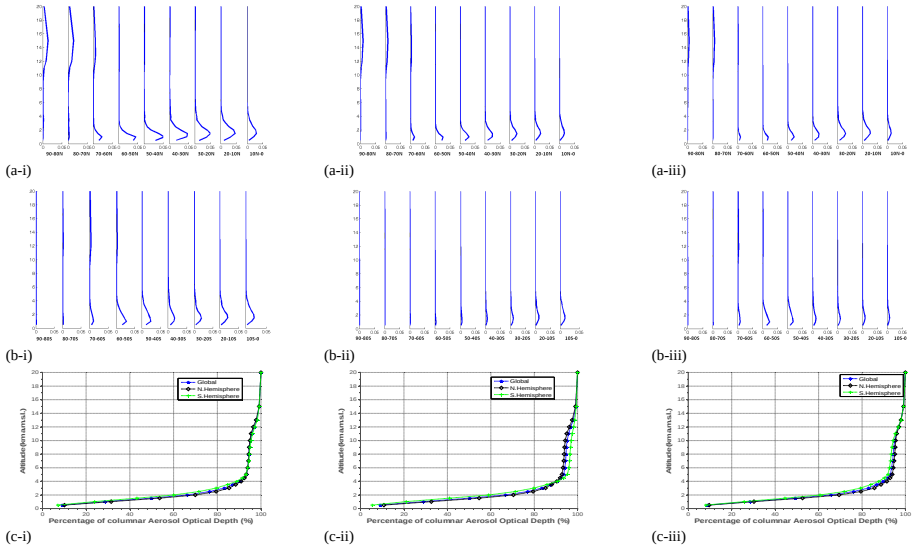

Fig. 7. Vertical distribution of HAC AOD per km for: total (left column, -i), fine (middle column, -ii) and coarse (right column, -iii). Results are given in terms of averages over 10-degree latitudinal zones of North Hemisphere (first row, **a**) and South Hemisphere (second row, **b**). In the third row **(c)**, is given the cumulative fraction of columnar AOD (in %) as function of altitude (in km) averaged over the two hemispheres and the globe.

ACPD
13, 5123–5163, 2013

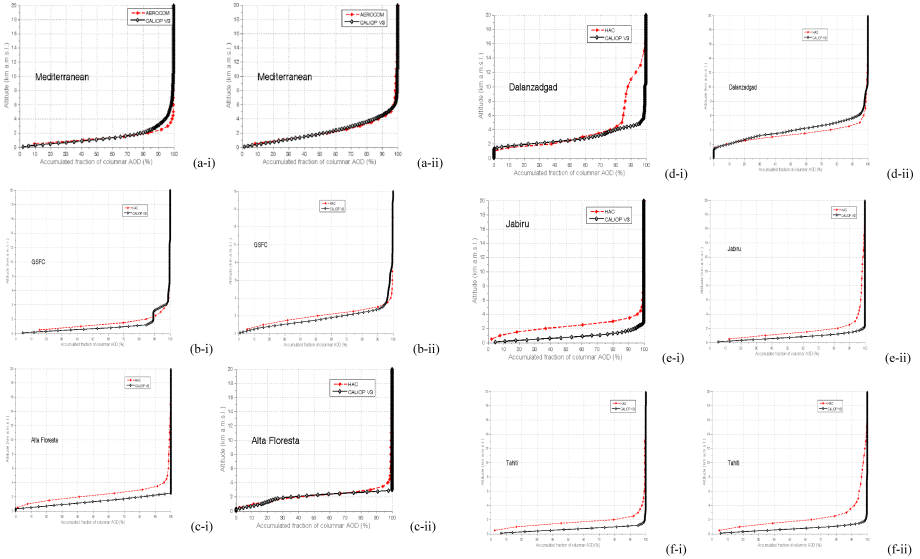

Fig. 8. Comparison between HAC (black lines and symbols) and CALIOP (red lines and symbols) vertical profiles of accumulated fractions of columnar total AOD. The comparison is made for: the Mediterranean basin **(a)**, and for the 5 selected world locations representative for specific aerosol regimes used in section 4 (**b** – GSFC, **c** – Alta Floresta, **d** – Dalanzadgad, **e** – Jabiru and **f** – Tahiti). Results are given separately for January (-i) and July (-ii), in each case. CALIOP values are for 532 nm, while HAC values are for 550 nm. Data for specific sites and for Mediterranean region are from July 2006 to January 2011.

ACPD
13, 5123–5163, 2013